ELSEVIER

Polymer 43 (2002) 2861–2867

polymer

www.elsevier.com/locate/polymer

Miscibility and interactions in poly(2,2,3,3,3-pentafluoropropyl methacrylate-*co*-4-vinylpyridine)/poly(*p*-vinylphenol) blends

H.L. Huang[a], S.H. Goh[a,*], A.T.S. Wee[b]

[a]*Department of Chemistry, National University of Singapore, 3 Science Drive 3, Singapore, Singapore 117543*
[b]*Department of Physics, National University of Singapore, 3 Science Drive 3, Singapore, Singapore 117543*

Received 12 November 2001; accepted 19 December 2001

Abstract

The miscibility and specific interactions in poly(2,2,3,3,3-pentafluoropropyl methacrylate-*co*-4-vinylpyridine) (PF*X*, $X = 0$, 28, 40 or 54, denoting the mol% of 4-vinylpyridine unit in the copolymer)/poly(*p*-vinylphenol) (PVPh) blends have been studied by differential scanning calorimetry (DSC), atomic force microscopy (AFM), Fourier transform infrared (FTIR) spectroscopy, and X-ray photoelectron spectroscopy (XPS). DSC studies show that PF0 is immiscible with PVPh, and the presence of a sufficient amount of 4-vinylpyridine units in the copolymer produces miscible blends. AFM images also clearly show that the blends change from heterogeneous to homogeneous upon the incorporation of 4-vinylpyridine unit into the copolymer. FTIR and XPS show the existence of inter-polymer hydrogen bonding between PF*X* and PVPh. The intensity of the inter-polymer hydrogen bonding increases with increasing 4-vinylpyridine content in the copolymer.

Keywords: Miscibility; Polymers blends; Specific interactions

1. Introduction

Fluorinated polymers possess many outstanding properties such as low surface energy and reduced coefficient of friction, which make them effective additives for modifying the surface properties of coating, adhesives, films, fibers and moldings [1–7]. For polymeric materials, the surface energy is determined mainly by the chemical structure at the surface. It is established that the surface energies of constituent groups decrease in the order CH_2 (36 mN/m) > CH_3 (30 mN/m) > CF_2 (23 mN/m) > CF_3 (15 mN/m) [8]. In particular, the $-(CF_2)_nCF_3$ groups in poly(fluoroalkyl methacrylate)s are effective in lowering the polymer surface energy [9].

However, the use of fluorinated polymers is often restricted due to their high manufacturing cost. In general, there are two methods to reduce the cost. Firstly, fluorinated monomers are copolymerized with non-fluorinated monomers to obtain copolymers with low surface energy [10–14]. Secondly, the expensive fluorinated polymers are blended with low-cost non-fluorinated polymers [15,16]. Because of the poor miscibility between fluorinated polymers and non-fluorinated polymers, it is difficult to use fluorinated homopolymers as additives especially when optical clarity of the materials is of importance. We have previously found that poly(fluoroalkyl methacrylate)s are less readily miscible with other polymers as compared to the corresponding poly(chloroalkyl methacrylate)s [17–20]. To promote miscibility between fluorinated and non-fluorinated polymers, comonomer units possessing suitable interacting groups can be incorporated into the fluorinated polymer via copolymerization. In this paper, we report the miscibility of poly(2,2,3,3,3-pentafluoropropyl methacrylate-*co*-4-vinylpyridine) (PF*X*, $X = 0$, 28, 40 or 54, denoting the mol% of 4-vinylpyridine unit in the copolymer) with poly(*p*-vinylphenol) (PVPh). The miscibility of the blends was examined by differential scanning calorimetry (DSC) and atomic force microscopy (AFM) while the underlying interactions were studied by Fourier transform infrared spectroscopy (FTIR) and X-ray photoelectron spectroscopy (XPS).

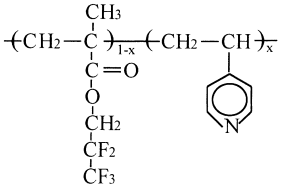

(a) PF*X*

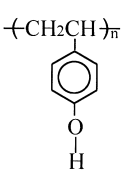

(b) PVPh

* Corresponding author. Tel.: +65-874-2844; fax: +65-779-1691.
E-mail address: chmgohsh@nus.edu.sg (S.H. Goh).

0032-3861/02/$ - see front matter
PII: S0032-3861(02)00069-1

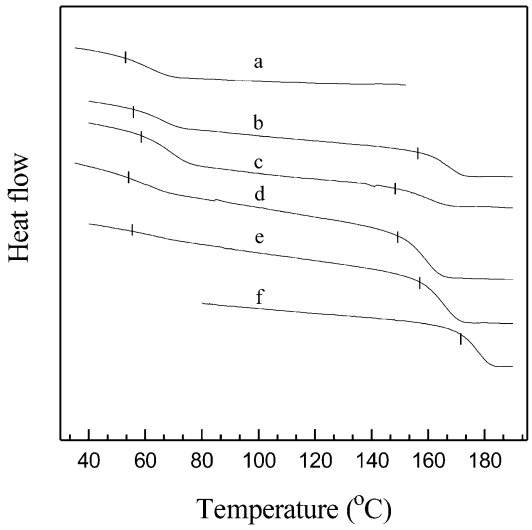

Fig. 1. DSC curves of PF0/PVPh blends containing (a) 100; (b) 80; (c) 60; (d) 40; (e) 20; (f) 0 wt% PF0.

2. Experimental

2.1. Materials

2,2,3,3,3-Pentafluoropropyl methacrylate and 4-vinylpyridine were purchased from Aldrich Chemical Co., Inc., and purified by distillation under a reduced pressure. Various PF*X* samples were synthesized by free radical copolymerization in tetrahydrofuran (THF) at 70 °C using 0.2 wt% 2,2′-azobisisobutyronitrile (AIBN) as initiator. PVPh ($M_w = 20$ kg/mol) and poly(4-vinylpyridine) (P4VPy) ($M_w = 300$ kg/mol) were purchased from Polysciences, Inc.

2.2. Preparation of blends

Appropriate amounts of polymers were separately dissolved in THF to form 2% (w/v) solutions. The polymer solutions were mixed and stirred for 24 h before being poured into Petri dishes where the solvent was allowed to evaporate slowly at room temperature. All the polymer blends were further dried in a vacuum oven at 60 °C for 2 weeks.

2.3. DSC measurements

The glass transition temperature (T_g) values of various samples were measured with a TA Instruments 2920 DSC using a heating rate of 20 °C/min. Each sample was subjected to at least three heating/cooling cycles to obtain reproducible T_g values. The initial onset point of the change of the slope in the DSC curve is taken to be the T_g.

2.4. AFM measurements

AFM measurements were performed using a METRIS 2001 atomic force microscope (Burleigh Instruments, Inc., USA). Height images were acquired under ambient conditions in contact mode using a silicon cantilever tip (ULTRASHARP™ cantilever length 200 μm and a resonance frequency of 21–44 kHz). Thin films used for AFM measurements were prepared by casting the THF solutions of polymer blends (1%, w/v) on 1 in. × 1 in. aluminum foil and dried at room temperature.

2.5. FTIR measurements

Infrared spectra were recorded on a Bio-Rad 165 FTIR spectrophotometer; 32 scans were signal-averaged at a resolution of 1 cm^{-1}. Samples were prepared by grinding the dried polymers or blends with KBr and compressing the mixtures to form disks. Spectra recorded at elevated temperatures were obtained by using a SPECAC high-temperature cell equipped with an automatic temperature controller.

2.6. XPS measurements

XPS measurements were carried out on a VG Scientific ESCALAB spectrometer using a Mg Kα X-ray source (1253.6 eV photons). Various samples were ground to fine powders and then mounted on a standard sample stud by means of a double-sided adhesive tape. The X-ray source was run at 12 kV and 10 mA. To compensate for surface charge effects, all core-level spectra were referenced to the C1s neutral carbon peak at a binding energy (BE) of 285.0 eV. The pressure in the analysis chamber was maintained at 10^{-8} mbar or lower during measurements. All spectra were obtained at a take-off-angle of 75° and curve-fitted with VGX-900I software.

3. Results and discussion

3.1. DSC characterization

The DSC curves of PF0/PVPh blends are shown in Fig. 1. All the curves exhibit two distinct glass transitions, indicating immiscibility. The lower T_g values are about the same as that of PF0, indicating that the phase is essentially pure PF0. On the other hand, the higher T_g values of the blends are about 10–20 °C lower than that of PVPh, showing the presence of PF0 in the PVPh-rich phase. Therefore, even though PF0 is not completely miscible with PVPh, there exists a weak interaction between PF0 and PVPh, leading to a limited extent of miscibility.

The DSC curves of PF28/PVPh blends are shown in Fig. 2. The existence of two glass transitions is seen in blends containing 90, 80, and 65 wt% of PF28. However, the T_g values deviate from those of the pure components, indicating a certain degree of interaction between the two polymers. Interestingly, the lower T_g values are even lower than that of PF28. Lu et al. [21] reported that the T_g values of miscible poly(styrene-*co*-vinylphenol dimethylsilanol)/poly(*N*-vinyl-2-pyrrolidone) (PVP) blends containing 10

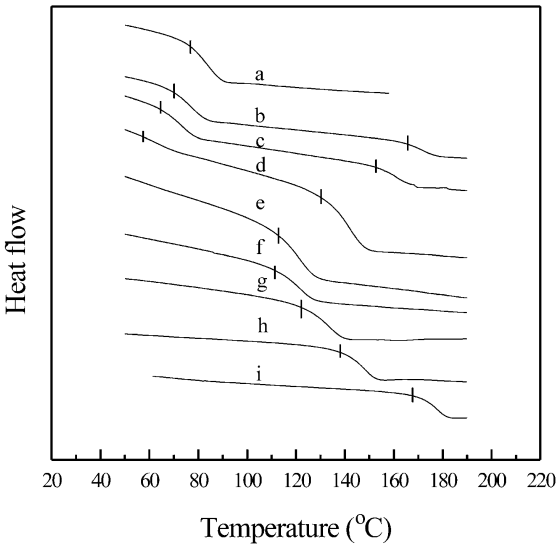

Fig. 2. DSC curves of PF28/PVPh blends containing (a) 100; (b) 90; (c) 80; (d) 65; (e) 50; (f) 35; (g) 20; (h) 10; (i) 0 wt% PF28.

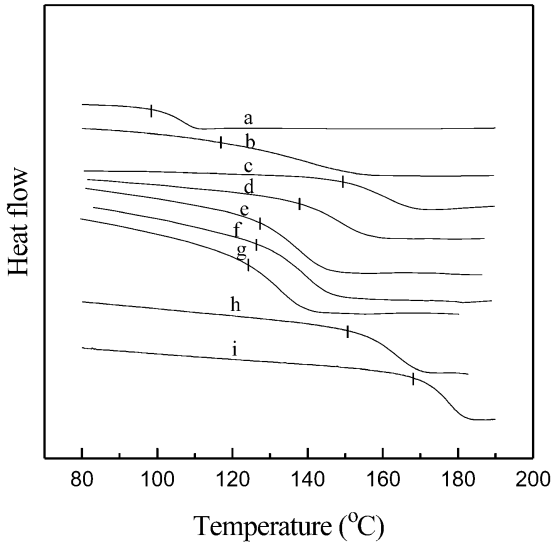

Fig. 4. DSC curves of PF54/PVPh blends containing (a) 100; (b) 90; (c) 80; (d) 65; (e) 50; (f) 35; (g) 20; (h) 10; (i) 0 wt% PF54.

and 20 wt% of PVP are lower than that of the low-T_g component. They suggested that the hydrogen bonding interaction was not extensive and thus the chain segments were poorly packed, giving rise to a large increase in free volume and a low T_g value. The weak interaction between PF28 and PVPh as well as the disruption of self-association of PF28 and PVPh could have contributed to the low T_g values. On the other hand, PF28/PVPh blends containing 50 wt% or less of PF28 show a single glass transition, indicating miscibility.

When the pyridine content in PF*X* is further increased to 40 mol%, the resulting PF40 is miscible with PVPh over the entire composition range as shown by the existence of a single glass transition in each blend (Fig. 3). It is noted that the glass transitions for PF40-rich blends are very broad. A broad glass transition in a miscible blend has been attributed to composition fluctuation in the blend which increases with decreasing affinity between the blend components and the fluctuation becomes macroscopic at the extreme limit of phase instability [22,23]. It has also been observed that there is an abrupt increase in the glass transition width just prior to the miscibility limit in a homopolymer/copolymer blend [24]. Thus the broadness of the glass transitions of these PF40/PVPh blends may be an indication that the blends are near the miscibility/immiscibility boundary. Nevertheless, a pyridine content of 40 mol% in PF*X* is sufficient to achieve miscibility with PVPh.

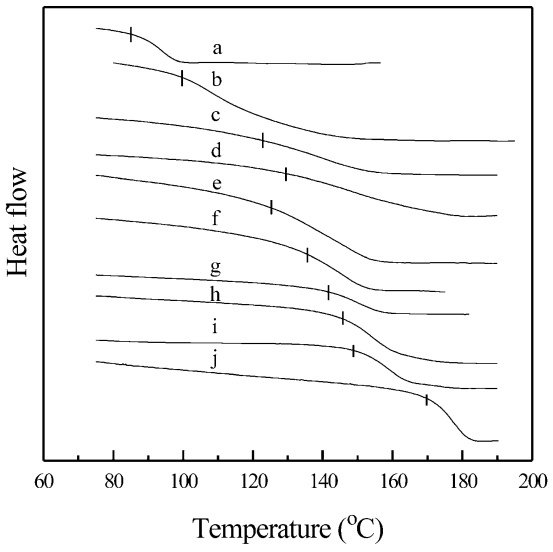

Fig. 3. DSC curves of PF40/PVPh blends containing (a) 100; (b) 90; (c) 80; (d) 65; (e) 50; (f) 35; (g) 20; (h) 10; (i) 5; (j) 0 wt% PF40.

The mixing of PF54 and PVPh led to the formation of gel-like materials. Since P4VPy and PVPh form complexes in suitable solvents [25,26], it is not surprising that PF*X* with a sufficiently high pyridine content could form complexes with PVPh as well. Thus the formation of gel-like materials between PF54 and PVPh indicates that the two polymers interact quite strongly with each other but not yet strong enough to precipitate out as a complex from the solution. The gels were difficult to separate by centrifugation and filtration. As such, the gels were dried to obtain transparent blends. As shown in Fig. 4, each PF54/PVPh blend shows a single glass transition and only the blend containing 90 wt% of PF54 shows a broad glass transition.

3.2. AFM characterization

Over the past decade, AFM has emerged as a powerful technique for imaging the blend surface [27–29]. The effect of hydrogen bonding interaction on the topographic features of blends can be clearly detected by AFM. Fig. 5 shows the

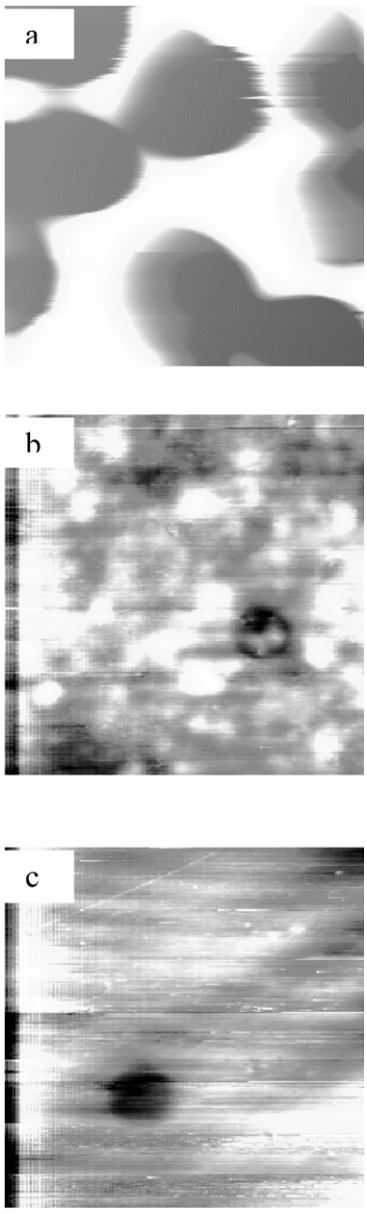

Fig. 5. AFM height images of (a) PF0/PVPh (20/80); (b) PF28/PVPh (20/80); (c) PF40/PVPh (20/80). The scan box is 22.5 μm × 23.8 μm. The height difference is 2.2 μm from the light to the dark region.

differences between the topographic features of PF0/PVPh, PF28/PVPh and PF40/PVPh blends. For the PF0/PVPh (20/80) blend (Fig. 5a), phase separation is clearly seen with a particle domain size of about 10 μm on the blend surface. The dark and light regions correspond to PF0 and PVPh, respectively. It is noted that although PF0 is the minor component in the blend, the surface enrichment of PF0 is clearly shown. In comparison, for the PF28/PVPh (20/80) blend (Fig. 5b), the phase separation is less distinct with a characteristic size smaller than 2 μm. For the PF40/PVPh (20/80) blend (Fig. 5c), the surface morphology appears homogeneous and it is not possible to detect accurately the phase boundary.

3.3. FTIR characterization

FTIR spectroscopy is used extensively in the study of polymer blends. This method is useful to detect the presence of interaction between various functional groups due to the sensitivity of the force constant to inter- and intra-molecular interactions. Pure PVPh is self-associated in the condensed state at ambient temperatures through the formation of intermolecular hydroxyl multimers. As shown in Fig. 6a, the hydroxyl band of pure PVPh consists of two components: a relatively narrow band at 3525 cm^{-1} for free hydroxyl groups and a broad band centered at 3370 cm^{-1} for a wide distribution of hydrogen bonded hydroxyl groups. The hydroxyl band of PVPh in the immiscible PF0/PVPh (80/20) blend is essentially the same as that of the pure PVPh, indicating that the interaction between PVPh and PF0 is very weak (Fig. 6b). For the PF28/PVPh (80/20) blend, which is deemed to be an immiscible blend by DSC, the shoulder band at 3525 cm^{-1} is still perceptible (Fig. 6c). However, a band at 3250 cm^{-1} appears to develop. For the PF40/PVPh (80/20) and PF54/PVPh (80/20) blends, the shoulder bands at 3525 cm^{-1} are difficult to observe, but the bands at 3250 cm^{-1} become more obvious (Fig. 6d and e). At the same time, bands at 3410 cm^{-1} are also apparent in the two spectra. The low-frequency band at 3250 cm^{-1} arises from interaction between the hydroxyl group and the pyridine nitrogen since the interaction between P4VPy and PVPh shifts the hydroxyl band to a lower frequency [26]. Thus the FTIR spectra reveals two types of interaction in the miscible PF*X*/PVPh blends, a weaker hydroxyl–hydroxyl interaction and a stronger hydroxyl–pyridine nitrogen interaction. At first glance, PF*X* does not appear to be self-associated at ambient temperatures. However, the high electronegativity of fluorine could make the vicinal hydrogen atoms in the

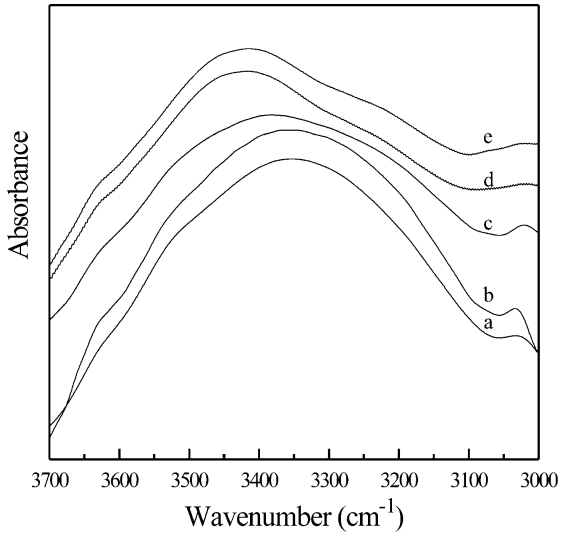

Fig. 6. FTIR spectra, recorded at room temperature, of the hydroxyl stretching band of (a) PVPh; (b) PF0/PVPh (80/20); (c) PF28/PVPh (80/20); (d) PF40/PVPh (80/20); (e) PF54/PVPh (80/20).

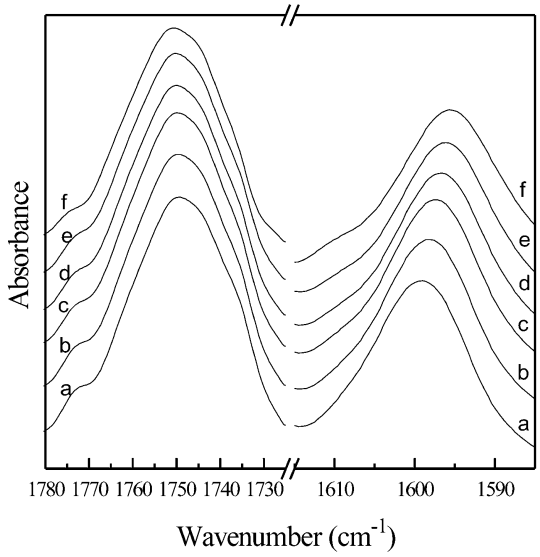

Fig. 7. FTIR spectra of the carbonyl stretching and the ring mode of pyridine group of PF40 recorded at (a) 30; (b) 60; (c) 90; (d) 120; (e) 150; (f) 180 °C.

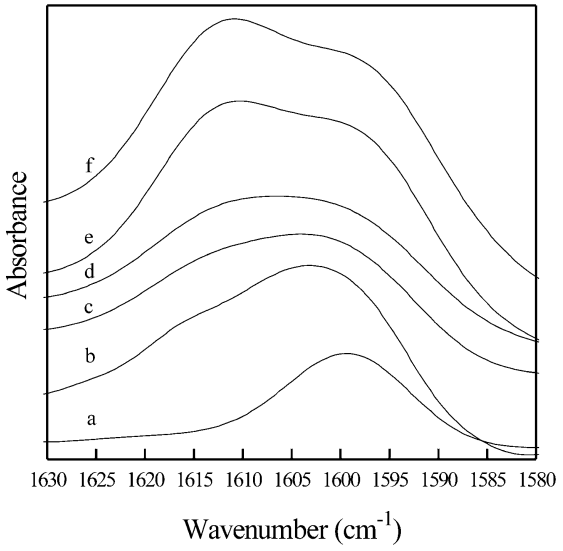

Fig. 8. FTIR spectra, recorded at room temperature, of the ring mode of pyridine group of PF40/PVPh blends containing (a) 100; (b) 80; (c) 65; (d) 50; (e) 35; (f) 20 wt% PF40.

$-CH_2CF_2CF_3$ group sufficiently acidic to form hydrogen bonding with a proton acceptor. In PF*X*, there are two possible proton-accepting sites: the carbonyl oxygen atom and the pyridine nitrogen atom. Fig. 7 shows the temperature-dependent infrared spectra of pure PF40 in the carbonyl stretching region around 1750 cm^{-1} and the pyridine ring mode around 1600 cm^{-1}. With increasing temperature, the carbonyl stretching band of PF40 at 1750 cm^{-1} remains practically unchanged. On the contrary, there is a gradual red shift in the ring mode of pyridine with increasing temperature. It is well established that both the carbonyl stretching band and the ring modes of pyridine are sensitive to hydrogen bonding formation. The ring modes shift to a high frequency when pyridine is hydrogen bonded to solvents such as water, ethanol and chloroform [30]. Similarly, when P4VPy undergoes hydrogen bonding interactions with proton-donating polymers, the ring modes also shift to a higher frequency and in some cases a new high-frequency band develops [31–33]. The change in the vibration frequency of the pyridine ring modes is attributed to an increase of the rigidity of the pyridine ring as a result of the involvement of the pyridine nitrogen atom in hydrogen bonding interaction [30]. Thus the low-frequency shift of the pyridine ring mode at 1600 cm^{-1} with increasing temperature is consistent with the disruption of the hydrogen bonding interaction between the pyridine nitrogen atoms and the vicinal hydrogens in $-CH_2CF_2CF_3$ group. Furthermore, the pyridine ring of PF40 vibrates at a higher frequency (1600 cm^{-1}) as compared to that of P4VPy (1597 cm^{-1}), indicating a higher rigidity of the pyridine ring in PF40.

Fig. 8 shows the FTIR spectra of the pyridine ring mode of various PF40/PVPh blends. As the PVPh content in the blend increases, a new band at 1611 cm^{-1} appears, indicating that the interaction between PF40 and PVPh is stronger than that of self-association of PF40. At the same time, the intensity of 1611 cm^{-1} band also increases with increasing PVPh content in the blend.

3.4. XPS characterization

The BE of a core-level electron depends on its chemical environment, and thus the XPS spectra provide information on specific interactions in polymer blends [34–36]. XPS studies have shown that the hydrogen bonding interaction between P4VPy and PVPh leads to the development of a new N1s peak with a BE value about 0.6–0.8 eV higher than that of the neutral N1s peak of P4VPy [34,36]. Fig. 9 shows the N1s core-level spectra of P4VPy, PF28/PVPh (65/35) and PF40/PVPh (65/35). The N1s spectrum of P4VPy shows a symmetric peak located at 399.3 eV. However, the N1s peaks of the two blends are broader than that of P4VPy and the peak maxima shift to a high-BE region. Each of the N1s spectra of PF*X*/PVPh blends can be curve-fitted with two component peaks with one remaining at 399.3 eV and another appearing around 400.0 eV. The appearance of the high-BE peak indicates that some of the pyridine nitrogen atoms interact with the hydroxyl groups of PVPh. As shown in Fig. 9b and c, the intensity of the high-BE N1s component peak increases with increasing 4-vinylpyridine content in PF*X*, indicating that more pyridine nitrogen atoms are involved in hydrogen bonding interaction with PVPh.

4. Conclusions

PF0 is immiscible with PVPh. In order to induce miscibility between the fluorinated polymer with PVPh, 4-vinylpyridine units were incorporated into the fluorinated

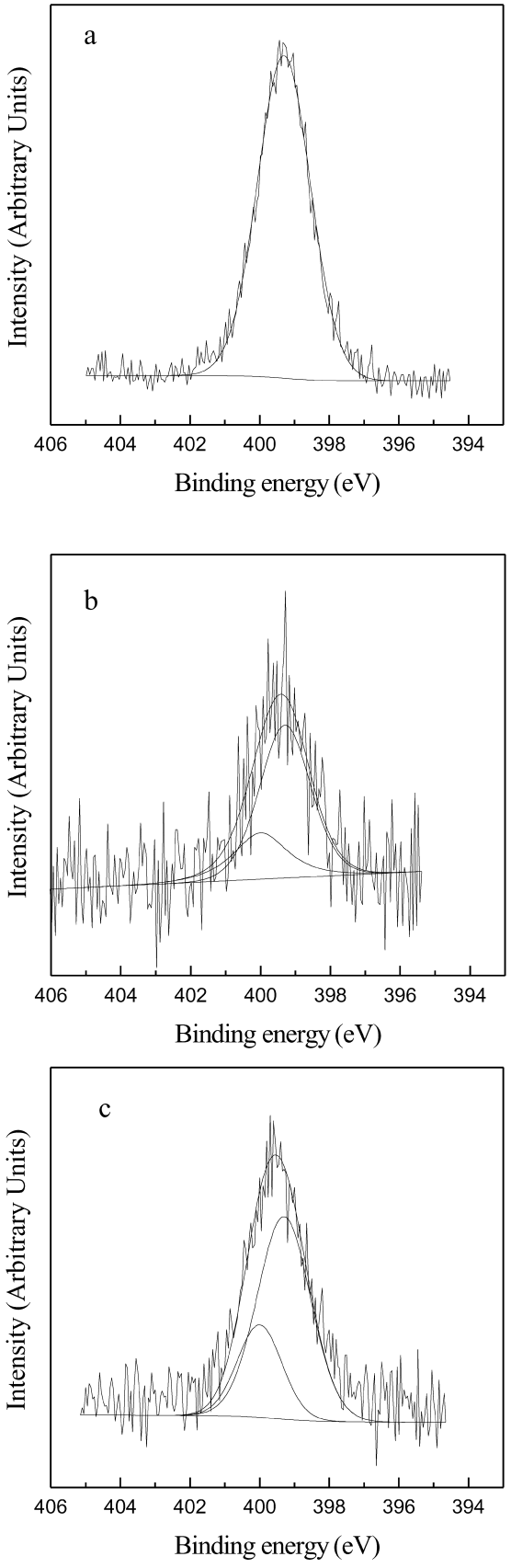

Fig. 9. XPS N1s core-level spectra of (a) P4VPy; (b) PF28/PVPh (65/35); (c) PF40/PVPh (65/35).

polymer by copolymerization. The high electronegativity of fluorine makes the vicinal hydrogen atoms in the $-CH_2CF_2CF_3$ group sufficiently acidic to form hydrogen bond with the pyridine nitrogen atoms, resulting in the self-association of PF*X* at ambient temperature. When PF*X* is blended with PVPh, inter-association between the pyridine group and hydroxyl group is present. For PF28, the hydrogen bonding is only strong enough to allow PVPh-rich blends to be miscible. On the other hand, PF40 and PF54 are miscible with PVPh over the entire composition range. AFM also confirms the improvement on the miscibility through the incorporation of 4-vinylpyridine unit in the fluorinated polymers as shown by a reduction in the domain size of PF*X* in the blend. Both FTIR and XPS show the existence of hydrogen bonding interactions between the hydroxyl groups of PVPh and the pyridine nitrogen atoms in PF*X*, and the inter-polymer interactions are stronger than the self-association of PVPh and of PF*X*. A study on the surface properties of the PF*X*/PVPh blends is in progress.

Acknowledgements

The authors thank the National University of Singapore for financial support of this research.

References

[1] Thomas RR, Lloyd KG, Stika KM. Macromolecules 2000;33:8828.
[2] Anton D. Adv Mater 1998;10:1197.
[3] Saegusa Y, Kuriki M, Kawai A, Nakamura S. J Polym Sci, Part A: Polym Chem 1994;32:57.
[4] Matsuda A, Kaneko T, Gong JP, Osada Y. Macromolecules 2000;33:2535.
[5] Castelvetro V, Ciardelli F, Francini G, Baglioni P. Macromol Mater Engng 2000;278:16.
[6] Shimizu T. Modern fluoropolymers. New York: Wiley, 1997. p. 507–23.
[7] Anolick C, Hrivnak JA, Wheland RC. Adv Mater 1998;10:1211.
[8] Tsibouklis J, Graham P, Eaton PJ, Smith JR. Macromolecules 2000;33:8460.
[9] Morita M, Ogisu H, Kubo M. J Appl Polym Sci 1999;73:1741.
[10] Park IJ, Lee SB, Choi CK. Macromolecules 1998;31:7555.
[11] Bongiovanni R, Malucelli G, Lombardi V, Priola A. Polymer 2001;42:2299.
[12] Kato S, Ueno Y, Kishida A, Miyazaki T. J Appl Polym Sci 1999;71:1049.
[13] Matsumoto K, Mazaki H, Nishimura R. Macromolecules 2000;33:8295.
[14] Toselli M, Messori M, Bongiovanni R. Polymer 2001;42:1771.
[15] Chen W, McCarthy TJ. Macromolecules 1999;32:2341.
[16] Pucciariello R, Villani V. Macromolecules 2001;34:1764.
[17] Peng J, Goh SH, Lee SY, Siow KS. Polymer 1994;35:1482.
[18] Peng J, Goh SH, Lee SY, Siow KS. Polym Networks Blends 1994;4:139.
[19] Peng J, Goh SH, Lee SY, Siow KS. Polym Networks Blends 1995;5:19.
[20] Peng J, Goh SH, Lee SY, Siow KS. Polym Adv Technol 1997;8:234.
[21] Lu S, Pearce EM, Kwei TK. Polymer 1995;36:2435.
[22] Woo EM, Barlow JW, Paul DR. J Appl Polym Sci 1985;30:4243.

[23] Fernandes AC, Barlow JW, Paul DR. J Appl Polym Sci 1986;32: 5481.
[24] Min KE, Paul DR. Macromolecules 1987;20:2828.
[25] Vivas de Meftahi M, Frechet JMJ. Polymer 1988;29:477.
[26] Dai J, Goh SH, Lee SY, Siow KS. Polym J 1994;26:905.
[27] Clarke S, Davies MC, Roberts CJ. Macromolecules 2001;34: 4166.
[28] Thomas RR, Lloyd KG, Stika KM, Stephans LE, Magallanes GS, Dimonie VL, Sudol ED, El-Aasser MS. Macromolecules 2000; 33:8828.
[29] Ton-That C, Shard AG, Teare DOH, Bradley RH. Polymer 2001;42:1121.
[30] Takahashi H, Mamola K, Plyler EK. J Mol Spectrosc 1966;21:217.
[31] Velada JL, Cesteros LC, Meaurio E, Katime I. Polymer 1995;36:2765.
[32] Velada JL, Cesteros LC, Katime I. Appl Spectrosc 1996;50:893.
[33] Cesteros LC, Meaurio E, Katime I. Macromolecules 1993;26:2323.
[34] Zhou X, Goh SH, Lee SY, Tan KL. Appl Surf Sci 1997;119:60.
[35] Chan CM, Weng LT. Rev Chem Engng 2000;16:341.
[36] Zeng XM, Chan CM, Weng LT, Li L. Polymer 2000;41:8321.